https://doi.org/10.5194/egusphere-2026-5292
Preprint. Discussion started: 9 September 2026

Estimates of sediment organic carbon burial and benthic-pelagic nutrient cycling in subarctic fjords (northern Nunatsiavut, eastern Canada)

Haley D. Geizer[1], Francesco Bisiach[2], Alexandre Normandeau[3], Maria Armstrong[1], Stephan Hamisch[4,5], Silas W. Jones[4], Casey R.J. Hubert[2], Kumiko Azetsu-Scott[6], Paul V.R. Snelgrove[4], Christopher W. Hunt[7], Michelle Saunders[8], Rodd Laing[8], Christopher K. Algar[1]

[1]Department Oceanography, Dalhousie University, Halifax, B3H 4R2, Canada
[2]Biological Sciences, University of Calgary, Calgary, T2N 1N4, Canada
[3]Geological Survey of Canada, Natural Resources Canada, Bedford Institute of Oceanography, Dartmouth, B2Y 4A2, Canada
[4]Department of Ocean Sciences and Biology Department, Memorial University, St. John's, A1C 5S7, Canada
[5]Alfred Wegener Institute, Helmholtz Centre for Polar and Marine Research, Bremerhaven, 27570, Germany
[6]Department of Fisheries and Oceans, Bedford Institute of Oceanography, Dartmouth, B2Y 4A2, Canada
[7]Ocean Process Analysis Laboratory, University of New Hampshire, Durham, New Hampshire, USA
[8]Nunatsiavut Government, Nain, BNL A0P 1L0, Canada

Correspondence to: Haley D. Geizer (haley.geizer@dal.ca)

Abstract

Fjords provide an important ecological service by burying and storing organic carbon (OC) more rapidly than most other marine environments. Quantifying this OC sink regionally requires an understanding of both the burial and remineralization processes that determine net OC sequestered. Within two sites from two Nunatsiavut fjords (Nachvak Fjord and Saglek Fjord, Labrador, Canada), we measured geochemistry associated with carbon, oxygen, and nutrient cycling and used a 1-D reactive transport model with an inverse modelling approach to simulate the geochemistry in the sampled sediment. A lower OC burial rate in sediment from Nachvak Fjord likely reflected significantly lower OC content in surface sediments and bottom sediments. Nachvak Fjord sediment modelling yielded a higher nitrification rate and a higher nitrate-dependent iron oxidation rate despite low heterotrophic denitrification compared to Saglek Fjord model results. Findings from microbial 16S rRNA gene sequencing were consistent with modelled biogeochemistry results from both fjords considering relative contributions from nitrate and sulfate reduction. Significantly higher OC content in Saglek Fjord sediments aligned with ~2X OC burial annually compared to Nachvak Fjord sediments. Differences in OC content and biogeochemical cycling might result from relative location chosen for sampling within each fjord, noting that we sampled outer fjord sediments in Nachvak Fjord, and inner fjord sediments in Saglek Fjord. Nevertheless, despite cold temperatures and good ventilation, both fjord basins utilized denitrification pathways (heterotrophic or nitrate-dependent iron oxidation) as the dominant nitrogen sink. Using both OC burial rates as end members, we estimate that northern Nunatsiavut fjords collectively store 8,000-33,000 tonnes OC yr^{-1}. Our

https://doi.org/10.5194/egusphere-2026-5292
Preprint. Discussion started: 9 September 2026

findings underscore the importance of additional studies with process-based measurements paired with OC burial estimates to understand further how climate change may alter benthic cycling and OC storage.

1 Introduction

Human-induced climate change is rapidly warming Arctic and subarctic environments, adding urgency to developing detailed modern carbon (C) budgets (AMAP, 2017; Atwood et al., 2020). As a critical component of the global C cycle, marine sediments sequester organic carbon (OC) for hundreds to thousands of years, which helps regulate climate (Iversen, 2022). Several studies have identified fjords as hotspots for OC accumulation and preservation (Smith et al., 2015; Smeaton & Autin, 2019; Bianchi et al., 2020). Organic matter (OM) in fjord sediments originates from sinking marine primary productivity or terrigenous sources delivered by surrounding water catchments (Cui et al., 2016). However, not all sediments sequester deposited OM. Microbial communities and benthic fauna convert some OM back into carbon dioxide (CO_2) and inorganic nutrients (nitrate: NO_3^-, nitrite: NO_x, phosphate: PO_4^{3-}, etc.) through the process of remineralization (Canfield et al., 1993; Glud, 2008). Quantifying this C sink requires understanding both the supply of OC to the seafloor and its degradation.

Fjords occur on historically glaciated coastlines where their steep walls and deep basins result in high sedimentation rates compared to other coastal settings (Smith et al., 2015; Faust & Knies, 2019; Bianchi et al., 2020). Low bottom currents and low oxygen concentrations in bottom water paired with high OC accumulation create a favourable environment for OC preservation (Smith et al., 2015; Bianchi et al., 2020). Hundreds of fjords occur in the Canadian Arctic and subarctic, with at least ~240 on Baffin Island alone (Syvitski et al., 2022), however, their seasonal ice cover and remote locations often make sampling difficult. Previous studies estimated that fjords globally store ~21-31 Mt of C annually, although this estimate did not incorporate heterogeneity of fine-grained sediments (Smith et al., 2015; Cui et al., 2016). Increased knowledge of fine-grained sediment in fjords lowered global estimates to ~5-10 Mt of OC annually (Smeaton and Austin, 2019). While neither of these calculations incorporated specific measurements from the Nunatsiavut region of Labrador, Canada, it is clear that burial models of OC storage must incorporate fjords as isolated depositional environments (Smith et al., 2015).

Studies that estimate OC stored in marine sediments often report burial efficiency (BE), defined as the percentage of OC buried at a specific sediment depth in relation to deposited OC (Bradley et al., 2022). Importantly, degradation occurs slowly beyond that depth (Canfield et al., 1993; Boudreau, 1997). Diagenetic modelling uses precise sediment-depth and sediment-age-resolved metrics that enable consistent evaluation of OC burial (Bradley et al., 2022). Additionally, these models can quantify the contributions of specific metabolisms or biogeochemical pathways to OC degradation, improving our understanding of nutrient and C cycling within a particular system (Boudreau, 1997). This nuance is critical with ongoing shifts in many environmental drivers in a warming climate.

https://doi.org/10.5194/egusphere-2026-5292
Preprint. Discussion started: 9 September 2026

Using a combined approach of observation, empirical flux measurements, and diagenetic modelling we explore 1) benthic-pelagic carbon and nutrient cycling in sediment from two northern Nunatsiavut fjords (58°N) and 2) estimate regional OC sequestration in northern Nunatsiavut fjords on a burial timescale of ~200 years.

2 Methods

2.1 Sampling sites

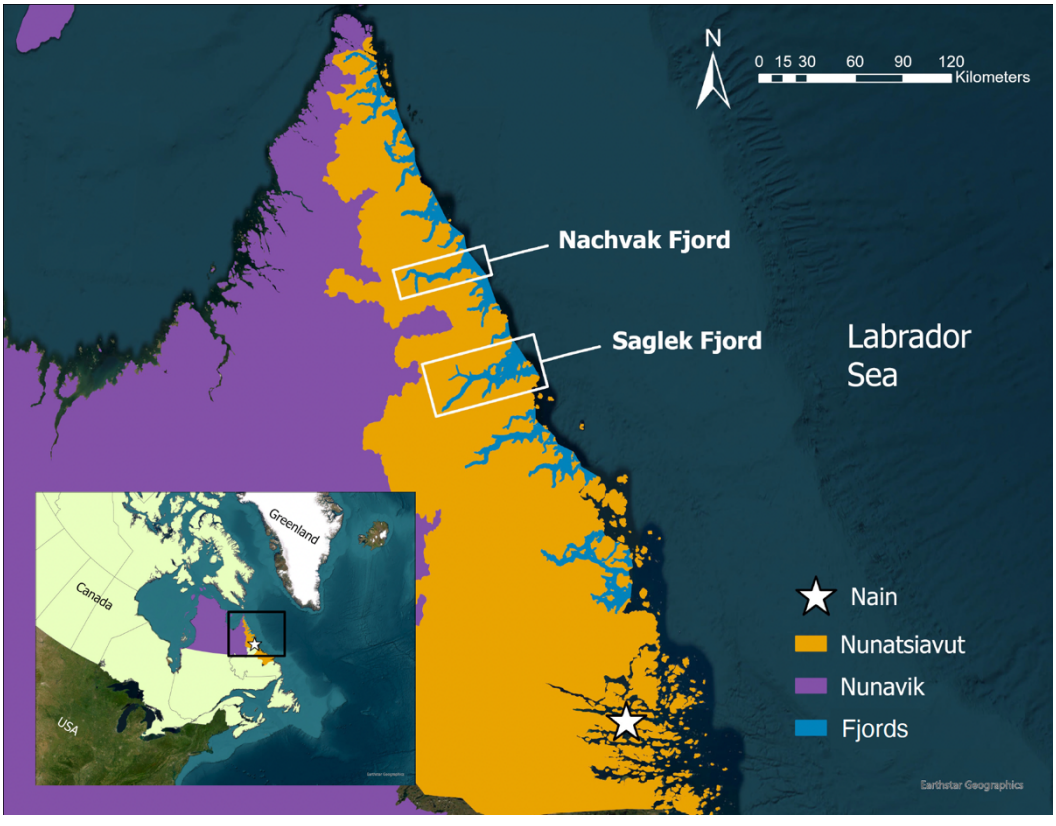

Figure 1. Nachvak and Saglek fjords, located along the Nunatsiavut coast in Labrador, Canada with northern fjords (n=18) shaded in blue.

Nachvak Fjord (59.07°N, 63.53°W) and Saglek Fjord (58.48°N, 63.22°W) are located within the Nunatsiavut coast, an Inuit governed region in Newfoundland and Labrador, Canada, and encompassing the Torngat Mountains National Park. This region may also be included in the proposed regional Torngat Marine Conservation area. Fjords in this area were formed by advancing and retreating glaciers during the Quaternary (Bell et al., 2009). Both Nachvak and Saglek fjords extend >40 km inland, with a maximum water depth in Saglek Fjord of ~300 m for its seven basins, in contrast to a seaward succession of 4 fjord basins in Nachvak Fjord that deepen from 90 m to 210 m. Semi-diurnal tidal currents likely play an important role in the dispersal of suspended sediment. The uninhabited Nachvak Fjord land mass and Ivitak Brook deliver most of its sediment deposits. Saglek

https://doi.org/10.5194/egusphere-2026-5292
Preprint. Discussion started: 9 September 2026

Fjord receives sediments primarily from Nakvak Brook, a feature with a larger catchment compared to Ivitak Brook. In this mountain range, 124 extant small mountain glaciers cover an area of ~21.8 km^2, though these have dramatically reduced since the Little Ice Age (Way et al., 2015). Calculated mass accumulation rates for both Nachvak and Saglek fjords, taking into consideration major basins, were estimated at ~39,000 t yr^{-1} and ~43,000 t yr^{-1} respectively, suggesting that sediment-gravity flows have contributed substantially to sediment transport (Bentley and Kahlmeyer, 2012).

Extreme and variable weather conditions in Torngat Mountains follow a subarctic regime mainly influenced by the Labrador Current (Banfield et al., 1998). Landfast sea ice forms along the entire northern Nunatsiavut coast in the winter (Davis et al., 2021). In recent decades, mean winter and summer temperatures in Nunatsiavut have increased by 2.0 and 0.5 ºC per decade respectively, resulting in noticeable environmental change (1987-2016; Barette et al., 2020). Both fjords abut alpine tundra, though shifts in temperatures have already led to changes in vegetation with increased shrub coverage (Davis et al., 2021; Fallu et al., 2022). Shrubs dominate (~70%) the land cover near Ivitak Brook, whose catchment feeds Nachvak Fjord, whereas primarily dry vegetation (~70%) dominates land cover around Nakvak Brook, which supplies Saglek Fjord (Davis et al., 2021). Increased shrub cover has elevated the OC reservoir in Arctic soils, likely influencing export of terrestrial OC to fjord basins (Sauerland et al., 2025). One study estimated that terrestrial sources provide 55-62% of OC buried in fjord sediments (Cui et al., 2016).

2.2 Core sampling

In September 2022 and July 2023, we collected box cores aboard the CCGS *Amundsen* in Nachvak and Saglek fjords (Figure 2), noting some differences in environmental conditions at each sampling site (Table 1). Upon retrieval, we immediately sub-sampled box cores using 6.7 cm-diameter core tubes that each penetrated to ~20 cm of sediment, leaving ~15 cm of overlaying water. Any water lost from the top of the box core during sampling was replaced with bottom water from the deepest Niskin bottle collected during a CTD/Rosette cast. We measured, photographed, and then left subcores undisturbed for ~12 hours in a 4°C cold room to re-establish natural chemical gradients that sampling may have disrupted. Bubbling cores with air during this time allowed cores to maintain oxygen (O_2) in in the overlying water. We then subdivided cores for onboard flux incubations (n=3), porewater extraction (n=2), O_2 microsensor-profiling (n=1). Another push core with a diameter of 10 cm was collected for ^{210}Pb dating (n=1).

https://doi.org/10.5194/egusphere-2026-5292
Preprint. Discussion started: 9 September 2026

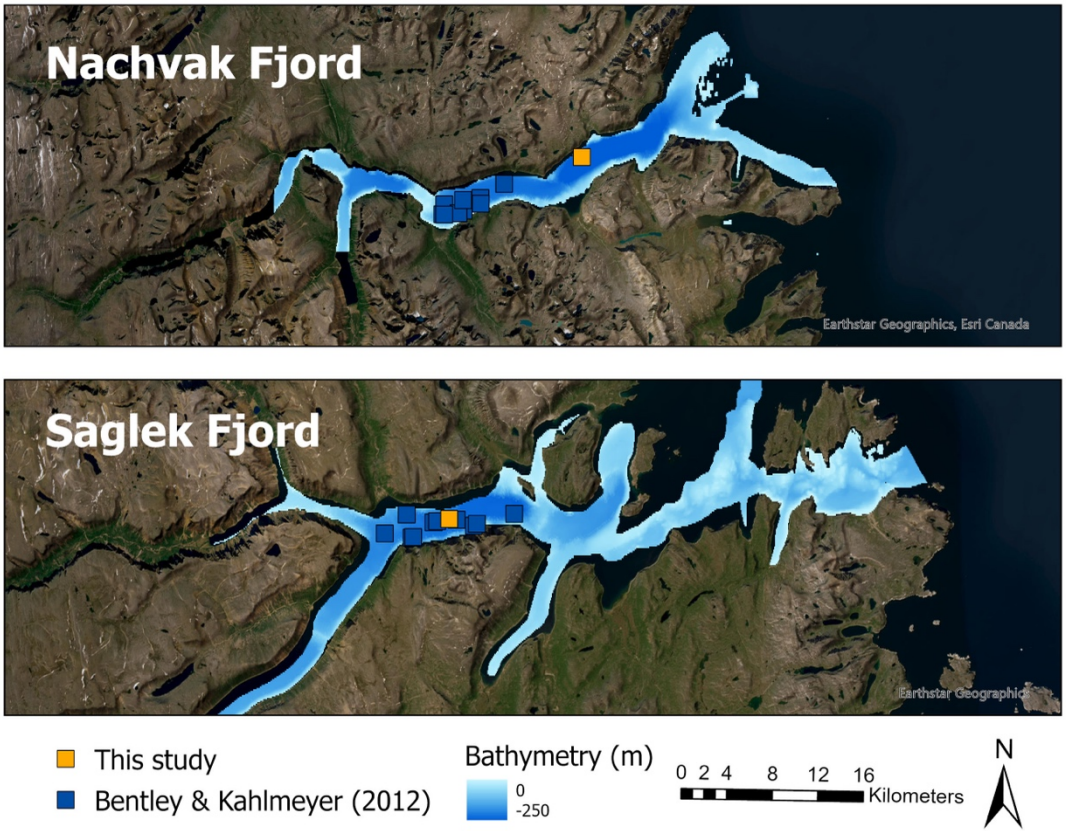

Figure 2. Locations of box cores sampled in Nachvak Fjord (n=1) and Saglek Fjord (n=1) in our study compared to box cores sampled in Bentley and Kahlmeyer (2012).

135

Table 1. Environmental conditions at sampling locations in Nachvak and Saglek fjords where Bw refers to bottom water.

Site	Date	Water depth (m)	Bw O_2 (% sat)	Bw salinity (psu)	Bw temp (°C)
Nachvak	Sept 22, 2022	192	66.4	32.9	-1.8
Saglek	July 23, 2023	240	67.1	32.2	-1.0

2.3 Incubation fluxes

140 We determined benthic fluxes of O_2 (TOU: total oxygen uptake), dissolved inorganic carbon (DIC), and nutrients (NO_3^-, NO_2^-, PO_4^{3-}, SiO_4^{4-}, NH_4^+) from ship-board incubations. To start the flux incubations, we replaced overlaying water with bottom water collected with a CTD/Rosette from that location, then capped the cores with airtight lids equipped with a spinning motor to ensure a well-mixed water column. During incubations of approximately 24 hours, we measured O_2 with sensor dots (SP-PSt3-NAU-D5-YOP) and a Fibox 4 optic oxygen meter (PreSens Precision Sensing GmbH, Regensburg, Germany). We also

https://doi.org/10.5194/egusphere-2026-5292
Preprint. Discussion started: 9 September 2026

collected and filtered (0.45 µm) water samples of ~30 mL for nutrients (~12 mL) and DIC (~15 mL), immediately replacing sampled water with bottom water. Additionally, we incubated a core tube with only seawater alongside our sediment cores at each site. We froze nutrient samples at -20°C and poisoned DIC samples with saturated mercuric chloride prior to storage at 4°C until analysis. O_2 measurements were taken every 2 h for the first 8 h and then in 8-h increments until the end of the experiment. DIC and nutrient samples were taken at 0 h, 8 h, 16 h and 24 h.

The CERC laboratory at Dalhousie University analyzed flux nutrient samples using a Skalar Continuous Flow Nutrient Analyzer. This instrument mixed samples with reagents and air bubbles, where the mixture was pumped and heated before entering a flow cell where colorimetric detection determined concentrations for the following species: NO_2^-, NO_3^-, PO_4^{3-}, SiO_4^{4-}, and NH_4^+ (McGrath et al., 2019). DIC measurements used an Apollo Scitech AS-C1 automated analyzer which acidified samples with 10% phosphoric acid and measured the produced CO_2 with a Li-core 6262 infrared gas analyzer (Hunt et al., 2014). We then calculated fluxes (reported in mmol m^{-2} d^{-1}) from the change in concentration in the overlying water during the course of the incubation according to

$$flux = \frac{dC}{dt} \times h \quad (1)$$

where C is concentration, t is time and h is the height of the water column.

2.4 Porewater extraction and analysis

Porewater extraction at 2 cm intervals used 0.15 µm Rhizon™ samplers inserted through pre-drilled holes (approximately 2 mm in diameter) along the side of the core liner. To extract porewater, we connected each Rhizon™ filter to a 10 mL acid washed syringe with a stopcock Luer lock fitting, which we used to collect ~8-10 mL of porewater samples that were sub-divided for measurements of DIC, Fe^{2+}, H_sS, NO_x, and NH_4^+. We added subsamples for Fe^{2+} to vials containing ferrozine reagent and fixed H_2S samples with zinc acetate, storing both at 4°C until analysis onshore. DIC samples were placed in 1.5 mL tubes filled completely with a well-formed meniscus to eliminate headspace prior to storing at 4 °C. We stored the remaining water in clean 15 mL falcon tubes at -20°C until remaining nutrient analyses onshore. Quantification of many of the porewater species of interest (NH_4^+, Fe^{2+}, H_sS) used a Thermo Scientific Evolution 201 UV-Visible Spectrophotometer (catalogue number: 840-210800) with established methods (Solórzano, 1969; Broenkow and Cline, 1969; Viollier et al., 2000). DIC samples were measured using the method noted above. Lastly, we measured NO_x^- porewater concentrations using a Thermolox NO_x Box by reducing NO_2^- and NO_3^- to NO using a mildly acidic vanadium (III) solution (Hendrix and Braman, 1995).

https://doi.org/10.5194/egusphere-2026-5292
Preprint. Discussion started: 9 September 2026

2.5 Microsensor O_2 profiling

At each sampling site, we collected 3-5 O_2 profiles from a single core using a UNISENSE field microprofiling system. This system consisted of a stepper motor that lowered a Clark-type electrode (UNISENSE OX-100) into the sediment at defined ~100 µm increments, until O_2 was depleted. Before the experiment, we calibrated the sensor with a two-point calibration using 100% O_2-saturated solution obtained by bubbling MQ water at in situ temperature for >10 mins, and an anoxic ascorbate solution. From the O_2 depth profiles, we observed the depth at which O_2 was completely consumed (O_2 penetration depth) and we estimated O_2 flux across the sediment water interface (DOU: diffusive oxygen uptake) using an in-house R script based on Berg et al. (1998).

2.6 Core sectioning and TOC

Upon completion of the flux incubations, we sectioned flux cores using a clean plastic plate to extrude the sediment into Ziplock bags. Incubation cores were sectioned at increments of 0-2 cm, 2-5 cm and then every 5 cm down the length of the core (n=3); sediment samples (12 samples total per fjord) were taken at the surface of each section for microbial community analysis by scooping sediment with a sterilized metal spatula into sterilized 2 mL plastic tubes, which we then froze at -80 °C. The rest of the sediment was placed in a clean Ziplock bag and frozen at -20 °C. For Nachvak Fjord, incubation core sections were also used to measure TOC content however Saglek Fjord's TOC content came from a single core sectioned at 2 cm increments down the length of the core.

At Dalhousie University, we thawed, homogenized and weighed ~10 g of sediment from each bag into clean glass scintillation vials. Samples were freeze-dried and ground with a metal spatula prior to fumigation with HCl. This latter step removed inorganic carbonates prior to measuring TOC (wt %) with a Shimadzu TOC-L Analyzer (Dickson et al., 2007).

2.7 ^{210}Pb analysis

We quantified sedimentation rate and bioturbation depths using ^{210}Pb. For Saglek Fjord, we sampled close to sites chosen by Bentley and Kahlmeyer (2012), allowing us to use their mean (n=10) sedimentation rate (Figure 2). Given the absence of such data for Nackvak Fjord in our sampling location, we collected an additional core for ^{210}Pb analysis, which we sampled every ~1 cm for the upper 10 cm and then every ~2 cm for the remainder. We then placed sediment sections in clean 60 mL falcon tubes and recorded their weights (g) prior to freeze-drying and reweighing. Samples were sent to INRS-ETE (Quebec City, Canada) for gamma counting to measure ^{210}Pb activity. Bioturbation depth was determined from the inflection point in the ^{210}Pb profile. Below this depth, we estimated sedimentation accumulation rates (S, cm yr^{-1}) from a least-squares fit to a constant flux constant sedimentation (CFCS) model,

https://doi.org/10.5194/egusphere-2026-5292
Preprint. Discussion started: 9 September 2026

$$A(z) = A(0)e^{-S/\lambda z} \quad (2)$$

where λ denotes the decay constant for the radionucleotide of interest (yr^{-1}) and A is the excess activity of ^{210}Pb (dpm g^{-1}) at depth z (Nittrouer et al., 1984).

2.8 16S sequencing and analysis

Genomic DNA extraction from sediment samples used the DNeasy PowerLyzer PowerSoil Kit (Qiagen, USA) and 0.4 g of sediment. Each batch of DNA extractions included a procedural blank using Milli-Q water instead of sediment. Resulting concentrations of DNA were determined with an Invitrogen Qubit 2.0 Fluorometer (Fisher Scientific, Canada).

We amplified a 291 bp fragment spanning the V4 and V5 regions of the 16S rRNA gene using primer pair 515-806R modified with Illumina MiSeq overhang adapters (Apprill et al., 2015). Each PCR reaction consisted of a 30-cycle program performed in triplicate. An initial denaturation step at 95°C for 5 min was followed by 30 cycles of denaturation at 95°C for 30 sec, annealing at 60°C for 45 sec, and extension at 72°C for 1 min. The program ended with a final extension at 72°C for 5 min. We validated PCR products, PCR blanks, and DNA blanks after each PCR run under a transilluminator following 1% agarose gel electrophoresis. Triplicate PCR products were pooled and purified using a NucleoMag NGS Clean-up and Size Select kit (Macherey-Nagel Inc., USA). A High Sensitivity DNA kit validated indexed products on an Agilent 2100 Bioanalyzer system (Agilent Technologies, Canada). We normalized indexed amplicons to an equimolar amount, which we loaded on a 96-well plate, and sequenced on an in-house Illumina MiSeq benchtop sequencer using Illumina's v3 600-cycle reagent kit to obtain 300 bp paired-end reads.

Primer and adapter trimming on raw reads used Cutadapt version 5.1 (Martin, 2011), followed by processing and analyzing trimmed libraries using RStudio (version 2025.05.0+496; Posit team, 2025) with R version 4.5.0 (R Core team, 2025). The DADA2 package (version 1.26.0) was used for filtering and ASV inference using default parameters and trimming read ends with scores below a value of 25 (Callahan et al., 2016). Taxonomy assignment used the SILVA database v138 (Quast et al., 2013). We used the *phyloseq* (version 1.42.0) and *vegan* (version 2.6.4) packages for statistical analyses on the quality-controlled reads including rarefaction and nMDS dissimilarity matrix (McMurdie and Holmes, 2013; Dixon, 2003). We then created relative abundance bar plots with the *dplyr* and *tidyr* packages from *tidyverse* collection (version 2.0.0; Wickham et al., 2019), and generated figures using the *ggplot2* package (version 3.5.1; Wickham, 2016). Metabolic potential within the microbial communities were inferred from the sequencing using the PiCRUST2 pipeline with default parameters (Douglas et

https://doi.org/10.5194/egusphere-2026-5292
Preprint. Discussion started: 9 September 2026

al., 2020), filtering results to obtain the weighted average of target genes indicative of the ability to perform sulfate reduction and nitrate reduction.

2.9 Calculating OC storage in each fjord

To calculate OC burial rates, the burial flux for each fjord (F_B: g OC m^{-2} yr^{-1}), we multiplied the mass accumulation rate (*MAR:* g sed cm^{-2} yr^{-1}) by the TOC content at the bottom of the sediment cores ($TOC_{deepest}$),

$$MAR = (1 - \theta) \times \rho_S \times S \quad (3)$$

$$F_B = MAR \times TOC_{deepest} \quad (4)$$

where θ is the porosity, ρ_S is sediment density in g cm^{-3} and S is the sedimentation rate in cm yr^{-1}.

Total OC sequestered (OC_{seq}) per fjord in tonnes OC yr^{-1} can be calculated using eq. 5,

$$OC_{seq} = F_B \times Ar \times m \quad (5)$$

where Ar is the fjord area (m^2) and m is the mud cover (%). We used an estimate of 30% mud cover based on Smeaton and Austin (2019) which can be adapted with regional habitat mapping data.

The initial amount of OC delivered to the seafloor (F_C) can be calculated with eq. 6 by adding the burial rate (F_B) with how much was lost through remineralization (R: DIC flux in g m^{-2} yr^{-1}).

$$F_C = F_B + R \quad (6)$$

Eq. 7 shows burial efficiency (*BE*), the percentage of OC that persists at a certain depth in the sediment (F_B) compared to the initial amount of OC delivered to the sediment (F_C).

$$BE = \frac{F_B}{F_C} \times 100 \quad (7)$$

2.10 Scaling up OC storage to northern Nunatsiavut fjords

We used eq. 5 to determine OC sequestration for all Nunatsiavut fjords. Because OC burial rates (F_B) between both fjords differed, the OC burial rate of Nachvak Fjord acted as a lower approximation whereas the OC burial rate of Saglek Fjord acted as an upper approximation giving us a range of OC buried and stored annually. We then multiplied those OC burial rates by the total Nunatsiavut northern fjord area.

https://doi.org/10.5194/egusphere-2026-5292
Preprint. Discussion started: 9 September 2026

To calculate the total area of northern Nunatsiavut fjords, we only considered areas from fjords north of Nain (north of latitude 57.157°N; see Figure 1). We opted for this strategy because we only have data from northern fjords, and fjords near Nain were difficult to identify because of the increasingly complex coastline. We defined a fjord as a channel perpendicular to the coast that becomes increasingly narrow approaching the head of the fjord. We estimated areas with ArcGIS Pro and the Nunatsiavut map shapefile (retrieved from open.canada.ca) by drawing a polygon connecting the mouth of each fjord overlapping with the Nunatsiavut map and deleting intersecting areas using the clip tool to leave outlines in the shape of each fjord (Figure 1). We then added the area of each outline together to yield a total Nunatsiavut northern fjord area of ~2830 km^2, only ~850 km^2 of which we considered to be characterized by fine-grained sediment.

2.11 Diagenetic modelling

We used a reactive transport model to partition C remineralization between the various redox remineralization pathways. The model was adapted from a previously developed diagenetic model established for the Bedford Basin in Halifax, Nova Scotia with full details of the model in Rakshit et al. (2025). Nine inorganic solutes were considered in this model: O_2, NH_4^+, NO_2^-, NO_3^-, Fe^{2+}, H_2S, SO_4^{3-}, CH_4, and DIC all modelled in µmol cm^{-3} and ten solid species: three pools of organic matter (highly, medium, and poorly reactive), three pools of iron (I, II, III) oxides (highly, medium, and poorly reactive $Fe(OH)_3$, $Fe(OH)_{3.MR}$, $Fe(OH)_{3.LR}$ respectively), two pools of MnO_2 (MnO_2 and $MnO_{2.MR}$), iron mono-sulfide (FeS) and pyrite (FeS_2). We modelled solid species in µmol cm^{-3} of dry sediment (expressed in wt% of dry sediment for plotting), setting the model domain at 50 cm in length with 100 grid layers that became increasingly thick with depth. Remineralization of particulate OC (POC) initially drove this model, yielding the consumption of O_2 and the production of NH_4^+ and CO_2. The movement of solutes and solids in the sediment was modelled with advection, compaction due to sedimentation, molecular diffusion, bioturbation and bioirrigation. The mass conservation equations for solutes and solids are given below,

$$\varphi \frac{\partial C_p(z,t)}{\partial t} = \frac{\partial}{\partial z}\left(\varphi D'(z) \frac{\partial C_p(z,t)}{\partial z} - \varphi u C_p\right) + \varphi \sum R + \varphi\gamma(C_{bw} - C(z,t)) \quad (8)$$

$$(1-\varphi) \frac{\partial C_s(z,t)}{\partial t} = \frac{\partial}{\partial z}(1-\varphi)(D_b(z) \frac{\partial C_s(z,t)}{\partial z} - v C_s + \Sigma R) \quad (9)$$

where φ is porosity, C_p and C_s are porewater (solute) concentration (µmol cm^{-3}) and dry weight percentage respectively, C_{bw} is the solute concentration in bottom water (µmol cm^{-3}), t is time, z is the vertical depth (cm), D_b is the bioturbation coefficient, u and v are advective velocities in sediment for porewater and solids respectively, ΣR is the sum of biogeochemical reactions, γ is the bioirrigation coefficient and D' is the tortuosity corrected diffusion coefficient (Boudreau, 1997).

$$D' = D_b + \frac{D}{1-2log\varphi} \quad (10)$$

https://doi.org/10.5194/egusphere-2026-5292
Preprint. Discussion started: 9 September 2026

3 Results

3.1 Sediment appearance

Sediment sampled from both fjords was consistently fine and soft. Grain size measurements from Bentley and Kahlmeyer (2012) indicate medium to fine silt sediments from both fjords with mean grain sizes of ~19 µm and ~22 µm for both Nachvak and Saglek fjords, respectively. They estimated bioturbation depths in Nachvak Fjord and Saglek Fjord of 6.2 ± 1.6 cm (n=10) and 5.1± 1.7 cm (n=10) respectively. The ^{210}Pb data shows a bioturbated depth of 4 cm (n=1) for sediment at our Nackvak Fjord sampling location (supplementary material). Mean porosity measured by Bentley and Kahlmeyer (2012) was 0.78 ± 0.02 (n=10) for Nachvak Fjord and 0.83 ± 0.06 (n=10) for Saglek Fjord. Mean sedimentation rates of Nachvak and Saglek fjords were 0.21 ± 0.1 cm yr^{-1} (n=11, including our core) and 0.26 ± 0.1 cm yr^{-1} (n=10) (Bentley and Kahlmeyer, 2012).

https://doi.org/10.5194/egusphere-2026-5292
Preprint. Discussion started: 9 September 2026

3.2 Sediment geochemistry

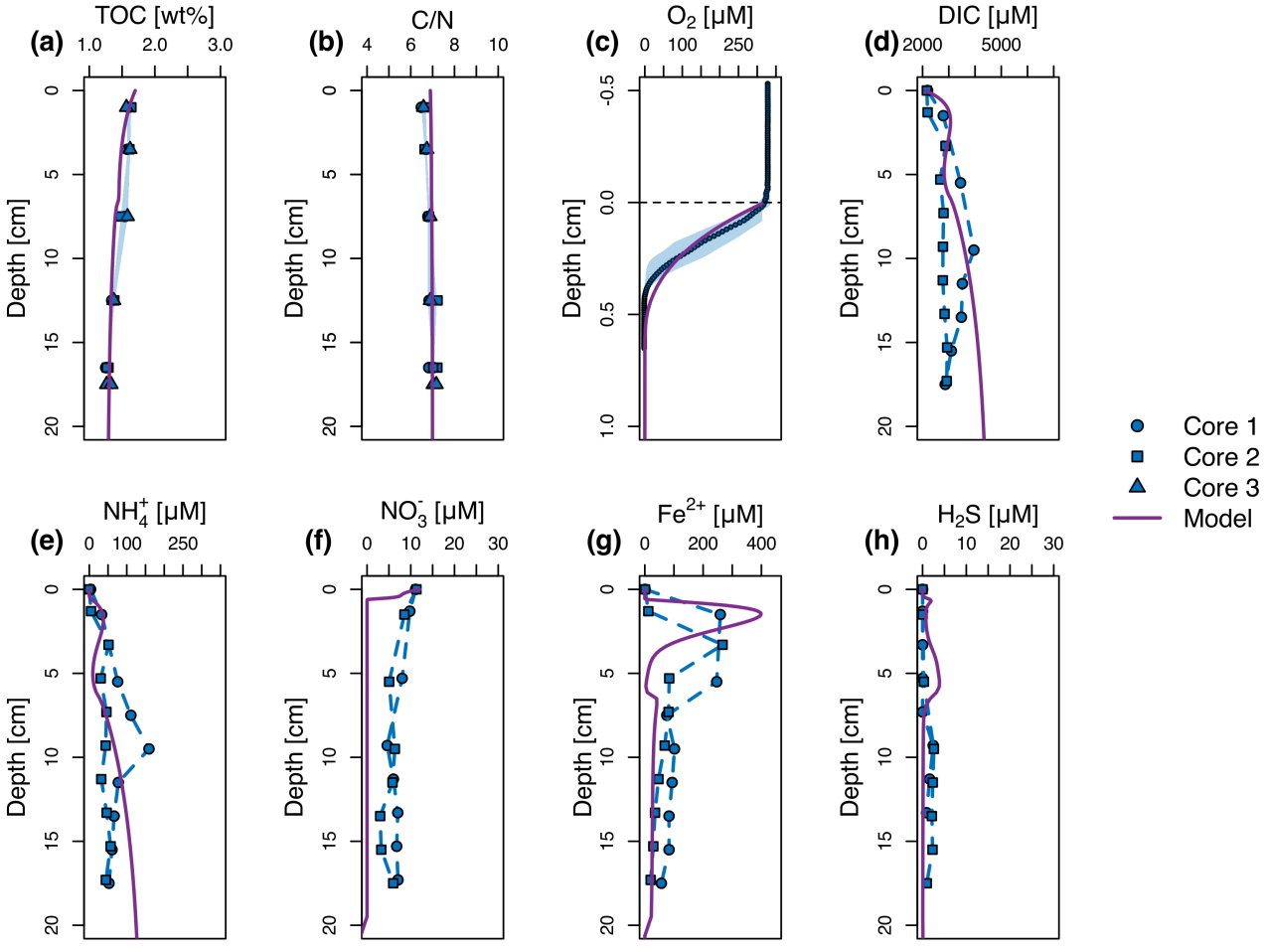

Figure 3. Depth profiles in Nachvak Fjord. Plots A-C show profiles in triplicate with blue shaded area representing the standard deviation among measured points. Plots D-H show duplicate porewater profiles. Purple lines indicate model simulations.

https://doi.org/10.5194/egusphere-2026-5292
Preprint. Discussion started: 9 September 2026

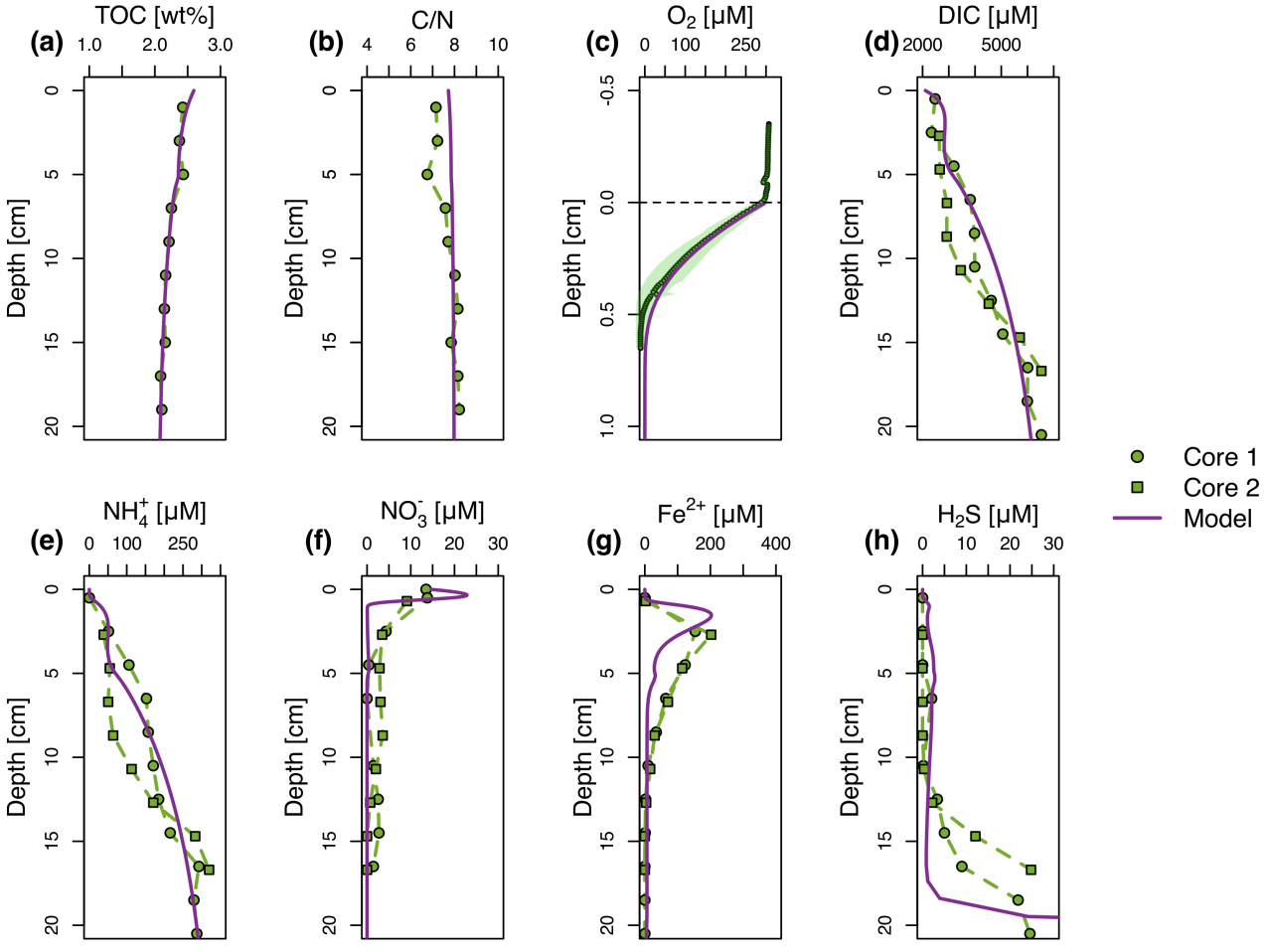

Figure 4. Depth profiles in Saglek Fjord. Plots A-B profiles are from a single core. Plot C is in triplicate with green shaded area representing the standard deviation among measured points. Plots D-H show duplicate porewater profiles. Purple lines indicate model simulations.

Sediment TOC content was lower in Nachvak Fjord sediment with ~1.6 wt% at the surface and decreasing to ~1.3 wt% at the bottom (Figure 4A), whereas Saglek Fjord surface sediment TOC was ~2.5 wt%, decreasing to ~2.1 wt% at depth (Figure 3A). Total nitrogen (TN) decreased with depth at both locations, though C/N ratios slightly increased with depth for both fjords (Figure 3B and 4B). The C/N ratio of organic matter varied between 6-8 for both fjords, suggesting an influence of OM from marine primary productivity (Meyers, 1994).

Oxygen penetration depths were 2.2 ± 0.8 mm and 3.3 ± 1.0 mm for Nachvak and Saglek fjords respectively and the sites did not differ significantly (t-test, p=0.3) (Figure 3C and 4C). DIC concentrations increased from near bottom water concentrations

https://doi.org/10.5194/egusphere-2026-5292
Preprint. Discussion started: 9 September 2026

at the surface to maximum values of ~4000 μM and ~6000 μM in bottom core samples for Nachvak and Saglek fjords, respectively (Figure 3D and 4D). NH_4^+ in porewater accumulated with sediment depth at both locations, although one of the Nachvak Fjord cores trended downward slightly after ~10 cm, a pattern mirrored in DIC porewater data. Maximum porewater NH_4^+ concentrations of ~150 μM in Nachvak Fjord compared to ~300 μM for Saglek Fjord (Figure 3E and 4E). NO_3^- porewater concentrations decreased from 10 μM to 5μM in Nachvak Fjord whereas Saglek Fjord porewater NO_3^- concentrations peaked at the surface at 15 μM, decreasing to 0 by 5 cm (Figure 3F and 4F). At both sites, Fe^{2+} concentrations peaked, by ~5 cm depth, but with higher values in Nachvak Fjord cores (~300 μM) than in Saglek Fjord cores (~200 μM) (Figure 3G and 4G). Saglek Fjord's Fe^{2+} concentrations as low as 0 μM contrasted Nachvak Fjord's Fe^{2+} concentrations of ~50 μM even at depth. Low H_2S concentrations (< 3 μM) characterized surface sediments for both fjords but with concentrations in Saglek Fjord cores as high as ~30 μM at depth (Figure 3H and 4H).

https://doi.org/10.5194/egusphere-2026-5292
Preprint. Discussion started: 9 September 2026

390

3.3 Benthic solute fluxes

Table 2. Sediment-water fluxes (mmol m^{-2} d^{-1}) for Nachvak Fjord (n=3) and Saglek Fjord (n=3) sediment cores.

Site	DOU	TOU	DIC	NH_4^+	NO_3^-	PO_4^{3-}	SiO_4^{4-}
Nachvak	-11.9 ± 2.4	-7.6 ± 1.4	10.7± 3.7	0.28 ± 0.23	-0.31 ± 0.003	0.003 ±0.02	4.4 ± 0.1
Saglek	-8.2 ± 3.3	-5.5 ± 1.3	7.20± 0.44	0.05 ±0.08	-0.04 ± 0.06	-0.003 ± 0.03	3.7 ± 1.2

395

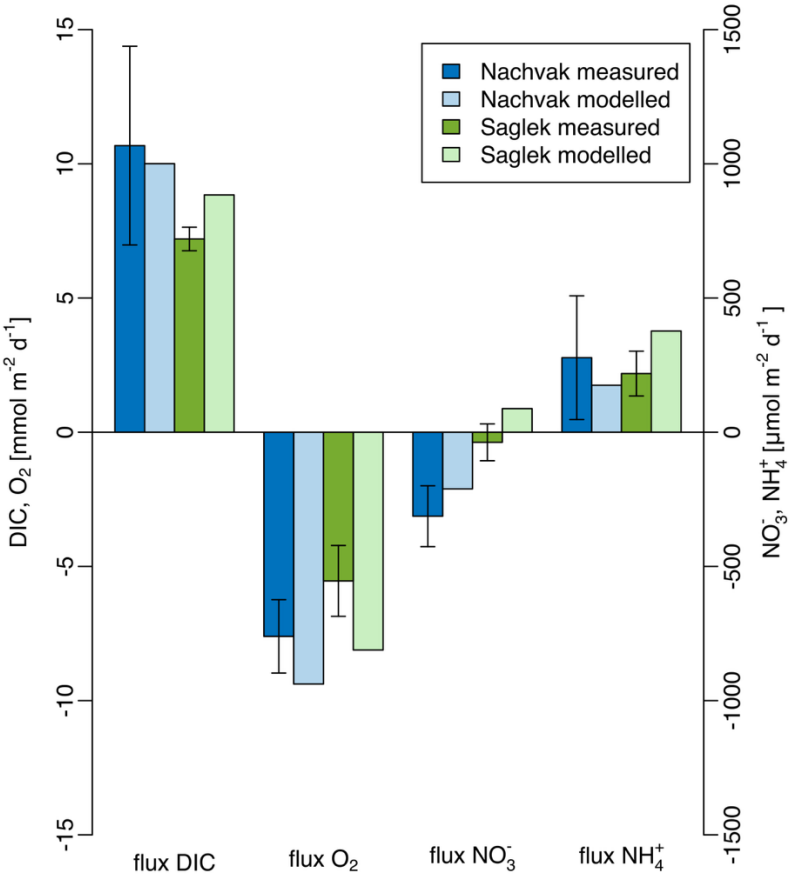

Figure 5. Measured benthic-pelagic fluxes in Nachvak Fjord (n=3, dark blue), modelled Nachvak Fjord flux results (light blue), observed fluxes in Saglek Fjord (n=3, dark green) and modelled Saglek Fjord fluxes (light green).

400

https://doi.org/10.5194/egusphere-2026-5292
Preprint. Discussion started: 9 September 2026

In terms of benthic-pelagic fluxes (Table 2, Figure 5), total oxygen utilization (TOU) (Nachvak: -7.6 -8.2 mmol m^{-2} d^{-1}, Saglek: -5.5-8.2 mmol m^{-2} d^{-1}) was slightly lower than DOU (Nachvak: -11.9 mmol m^{-2} d^{-1}, Saglek: -8.2 mmol m^{-2} d^{-1}), likely because we bubbled cores during profiling thus increasing the sediment-water interface oxygen gradient. DOU (t-test, p=0.5) and TOU (t-test, p=0.2) fluxes did not differ significantly between Saglek Fjord and Nachvak Fjord. DIC efflux for both sites of 10.68 ± 3.70 mmol DIC m^{-2} d^{-1} and 7.20 ± 0.44 mmol DIC m^{-2} d^{-1} for Nachvak Fjord and Saglek Fjord respectively differed significantly (t-test, p=0.008).

A principal component analysis comparing benthic-pelagic fluxes from both sites (Figure 6) showed that PC1 and PC2 explained 85.5% of the variance and that triplicate samples clustered by site. PCA loadings inform gradients associated with each axis, in that the magnitude of O_2 and DIC fluxes explained PC1 whereas PC2 depended on NH_4^+ and SiO_4^{4-} cycling. Varying Nachvak Fjord fluxes along the PC2 axis suggest higher O_2 and DIC fluxes and that NH_4^+ and SiO_4^{4-} cycling explained most variance between cores. The opposite pattern emerged for Saglek Fjord fluxes, where most variance occurred along the PC1 axis; this pattern suggests greatest influences by DIC and O_2 flux variation. The PERMONOVA value of 0.8 likely reflected small sample size though we observed a clear separation between benthic-pelagic cycling between sites.

.

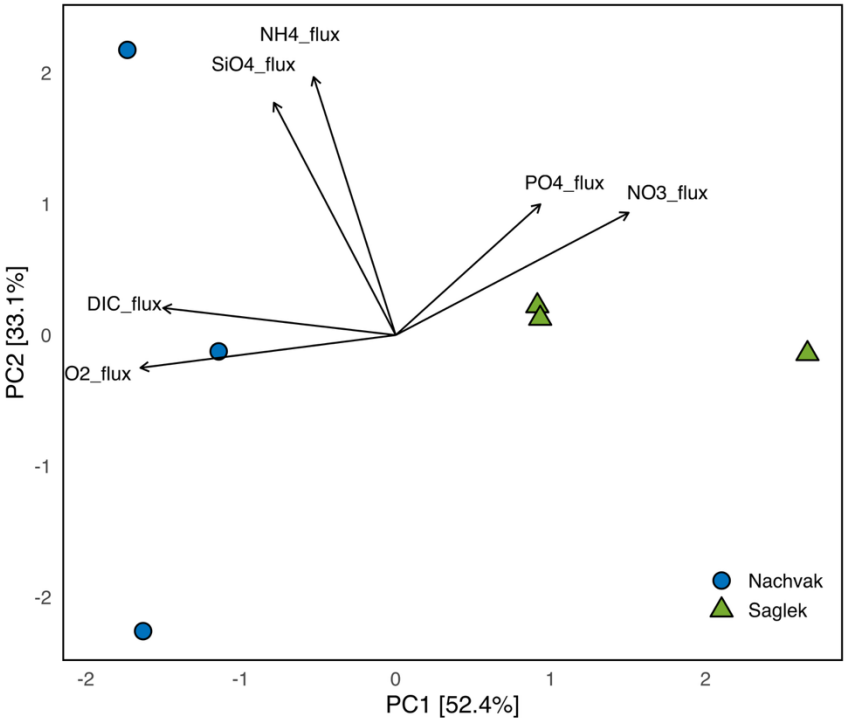

Figure 6. Principal component analysis (PCA) of benthic solute fluxes measured in surface sediments from Nachvak and Saglek fjords based on six variables (DIC, O_2, NH_4^+, NO_3^-, PO_4^{3-}, and SiO_4^{4-} fluxes) scaled prior to analysis.

https://doi.org/10.5194/egusphere-2026-5292
Preprint. Discussion started: 9 September 2026

3.4 Model results

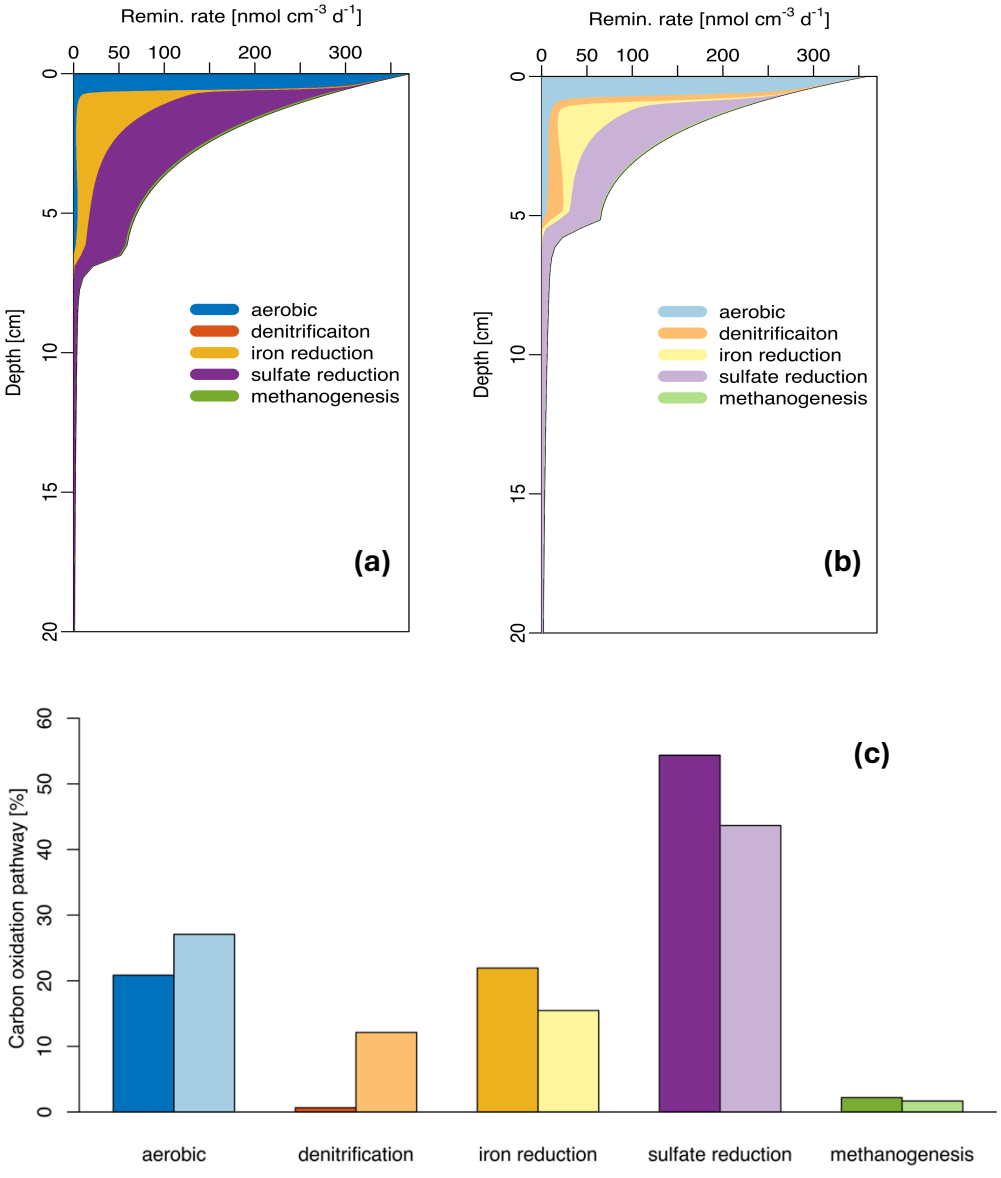

Figure 7. Modelled benthic remineralization rates with depth in sediment from Nachvak Fjord (a) and Saglek Fjord (b) with the responsible C degradation pathways and their weighted contribution (c), where dark shades represent Nachvak and light shades represent Saglek.

https://doi.org/10.5194/egusphere-2026-5292
Preprint. Discussion started: 9 September 2026

The reactive transport model reproduced porewater solutes and sediment TOC concentrations for both Saglek and Nachvak fjords accurately except for the C/N ratios of solid OM which were slightly overestimated at the surface for both sites (Figures 3A and 4A). Porewater concentration and benthic-pelagic flux simulations for both sites provided an internal check on the consistency of measurements on cores. In addition to measurement validation, we used our model to partition remineralization rates between the distinct electron acceptors that correspond to metabolic function (Figure 7).

Modelled rates of OC remineralization were 10.0 mmol C m^{-2} d^{-1} and 8.7 mmol C m^{-2} d^{-1} for Nachvak and Saglek fjords, respectively. Using the model, we separated the contributions of C degradation into the responsible metabolisms. Sulfate reduction dominated Nachvak Fjord sediment metabolism (54.5%) with little C degradation from heterotrophic denitrification (0.4%) (Figure 7). Sulfate reduction also dominated Saglek Fjord sediment metabolism (43.2%) with our model attributing ~13.5% of C degradation to heterotrophic denitrification (Figure 7).

3.5 16S rRNA gene sequencing results

We obtained a total of 1,647,018 processed amplicon sequence variants across the 24 sediment samples we sequenced, providing a depth-resolved assessment of microbial biodiversity from both fjords. Taxonomic assignment of these 16S rRNA gene sequences revealed a high relative abundance of sequences assigned to chloroplasts rather than a bacterial lineage (see supplementary material) The prevalence of these sequences varied substantially across samples, ranging from 4-30 % of all processed reads, likely reflecting the presence of dead or living eukaryotic phototrophs in the sediment. Samples from both fjords varied widely in the proportion of recovered chloroplast sequences. For Nachvak Fjord, on average 21% of mapped sequences were assigned to chloroplasts compared to 6% for Saglek Fjord. Given that chloroplasts are not free-living organisms capable of metabolism, these sequences were excluded from the non-metric multidimensional scaling ordination analysis used to compare the two samples.

https://doi.org/10.5194/egusphere-2026-5292
Preprint. Discussion started: 9 September 2026

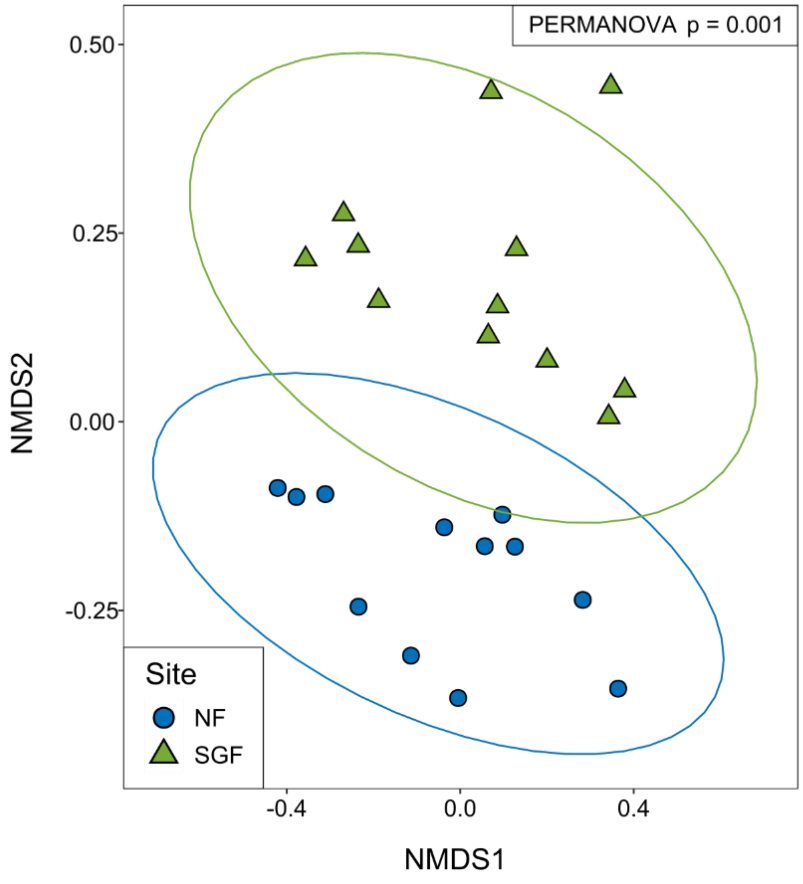

Figure 8. Non-metric multidimensional scaling (nMDS, stress = 0.15) ordination plot based on a Bray-Curtis dissimilarity matrix illustrating differences in microbial community composition between Nachvak Fjord (blue circles) and Saglek Fjord (green triangles) sediments. Each point represents the microbial community of a single depth horizon (0, 2, 5, and 10 cm) from an individual sediment core, as characterised by 16S rRNA gene amplicon sequencing post removal of chloroplast amplicons. Ellipses represent 95% confidence intervals around each site grouping. Community composition differed significantly between sites (PERMANOVA, $F_{1,22} = 5.22$, $R^2 = 0.19$, $p = 0.001$, 999 permutations).

Microbial community composition differed significantly between the two fjords. This dissimilarity was more marked prior to the removal of chloroplasts amplicons from the libraries but remained significant even after their exclusion (PERMANOVA, Bray–Curtis, $R^2 = 0.19$, $p = 0.001$) (Figure 8).

https://doi.org/10.5194/egusphere-2026-5292
Preprint. Discussion started: 9 September 2026

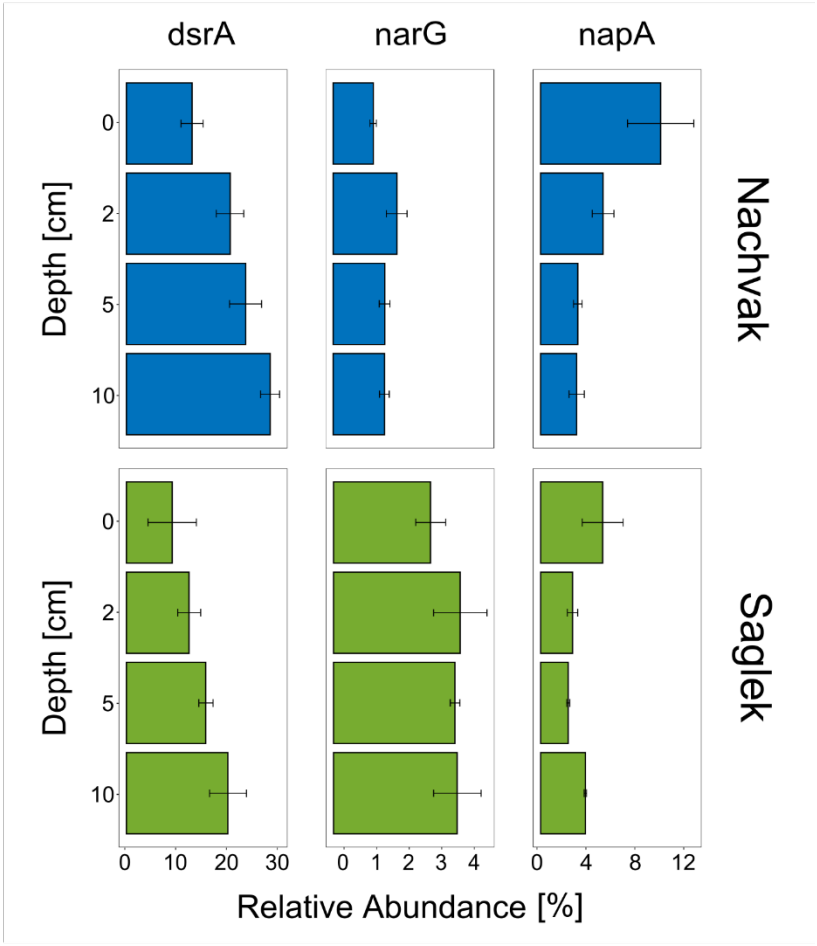

Figure 9. Weighted mean relative abundance (%) of prokaryotic genomes predicted to carry the sulfate reduction gene *dsrA* and the nitrate reduction genes *narG* and *napA* across sediment depth horizons (0, 2, 5, and 10 cm) in Nachvak Fjord (blue) and Saglek Fjord (green). Gene abundance was inferred using the PiCRUST2 functional gene prediction pipeline. Error bars represent ± one standard deviation across three environmental replicates. Note that x-axis scales differ between genes.

Functional gene prediction using PiCRUST2 revealed differences in the metabolic potential of the microbial communities between the two fjords. Nachvak Fjord sediment is predicted to have a higher proportion of genomes capable of sulfate reduction, with a predicted mean of 21 ± 6 % of the microbial community carrying the *dsrA* gene across all depths, compared to 14 ± 5 % in Saglek Fjord (Figure 9). In both fjords, the relative abundance of predicted sulfate reducers increased with sediment depth, with the 10-cm-deep sediment indicating more than double the proportion of predicted *dsrA* compared to surface sediment (Figure 9). For nitrate reduction, Saglek Fjord data predicted a higher proportion of genomes carrying the cytoplasmic nitrate reductase gene *narG* (3 ± 0.4 %), but no clear trend with sediment depth (Figure 9). In contrast, the

https://doi.org/10.5194/egusphere-2026-5292
Preprint. Discussion started: 9 September 2026

periplasmic nitrate reductase gene *napA* is predicted to be more prevalent in Nachvak Fjord sediments (5 ± 3 %), primarily within the uppermost 2 cm of sediment (Figure 9).

3.6 OC burial estimate

We estimate Nachvak Fjord receives 62.7 ± 18.0 g OC m^{-2} yr^{-1}, and of this OC, sediments remineralize 46.8 ± 16.3 g OC m^{-2} yr^{-1} while burying 15.9 ± 7.7 g OC m^{-2} yr^{-1} below the active layer, resulting in a burial efficiency of ~26%. Saglek Fjord, in contrast, receives 56.8 ± 10.1 g OC m^{-2} yr^{-1}, of which sediments remineralize 31.6 ± 1.9 g OC m^{-2} yr^{-1} and bury 25.2 ± 9.9 g OC m^{-2} yr^{-1}, yielding a burial efficiency of, ~44%. Assuming both sites are representative of their respective fjords and that fine grained sediment cover 30% of the area, similar to observations for mid-latitude Scottish and Irish fjords (Smeaton and Austin 2019), we calculate that Nachvak Fjord (total area: 190 km^2) sequesters an estimated 900 ± 430 tonnes OC yr^{-1} and Saglek Fjord (total area: 245 km^2) sequesters nearly twice as much at 1850 ± 730 tonnes OC yr^{-1}; these rates differ significantly (t-test, p=0.009). The larger area and higher burial efficiency drive greater sequestration in Saglek Fjord. Our model calculated an OC deposition rate of 59.6 g OC m^{-2} yr^{-1}, a remineralization rate of 44.0 g OC m^{-2} yr^{-1} and a burial rate of 15.6 g OC m^{-2} yr^{-1} for Nachvak Fjord. Model results suggest Saglek Fjord receives 65.5 g OC m^{-2} yr^{-1}, remineralizes 38.4 g OC m^{-2} yr^{-1} and buries 27.0 g OC m^{-2} yr^{-1}. Modelled rates for both fjords aligned well with measured rates.

Finally, assuming per area burial rates for Nachvak and Saglek fjords are comparable to upper and lower bounds for all northern Nunatsiavut fjords, the 18 fjords indicated by the blue shading in Figure 1, which collectively encompass ~850 km^2 of fined-grained sediment, we estimate that they may sequester 8,000-33,300 tonnes OC yr^{-1}. Using our model domain of 50 cm and assuming constant sedimentation rates at each site, OC buried annually can be sequestered on a timescale of at least ~200 years (Figure 10).

https://doi.org/10.5194/egusphere-2026-5292
Preprint. Discussion started: 9 September 2026

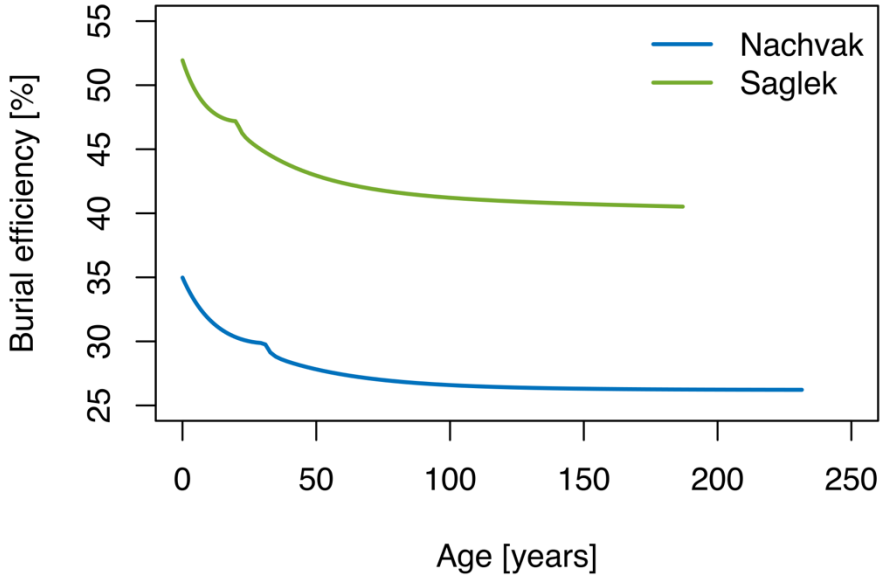

Figure 10. Modelled burial efficiencies with sediment age based on a sediment depth of 50 cm in both Nachvak Fjord and Saglek Fjord sediments.

https://doi.org/10.5194/egusphere-2026-5292
Preprint. Discussion started: 9 September 2026

4 Discussion

Data from this study suggests Saglek Fjord sediments may store ~2X more OC annually compared to Nachvak Fjord. This elevated OC storage in Saglek Fjord likely reflects higher TOC in surface and bottom sediments and a larger fjord area (~245 km^2 compared to ~190 km^2 for Nachvak Fjord). The OC content measured in surface sediments in our study (Nachvak: ~1.6%, Saglek: ~2.5%) greatly exceed the estimated average OC content (0.7%) in surface sediments from other Eastern Canada fjords (Smith et al., 2015). Similar C/N ratios for both fjords (~6-8) suggest that we cannot attribute greater TOC in our Saglek Fjord sediment samples to a difference in OM source (i.e., terrestrial vs marine), though potential OM sources merit further consideration. Previous work reports variable correlations between TOC and grain size in fjords but report higher TOC concentrations in fjord basins (Smeaton and Austin, 2019). Although the Nachvak Fjord sampling site was within a basin, circulation with the open ocean may not be as restricted (i.e., no outer sill) which could affect the trapping of particles (Figure 2). Lower TOC can characterize sediments closer to fjord mouths (Cui et al., 2016; Duffield et al., 2017), but this scenario depends on mineral dilution and OC source. Line (2016) measured surface TOC in inner fjord Nachvak Fjord sediments and reported TOC concentrations similar to Saglek Fjord sediments in our study (>2%). We may underestimate OC storage in Nachvak Fjord and overestimate OC storage in Saglek Fjord, noting documented heterogeneity in fjord OC and sedimentation rates (Smeaton and Austin, 2019). Nevertheless, inclusion of multiple sites that span inner and outer fjord sediments, even from different fjords, would improve the accuracy of total northern Nunatsiavut muddy sediment OC stock estimate.

https://doi.org/10.5194/egusphere-2026-5292
Preprint. Discussion started: 9 September 2026

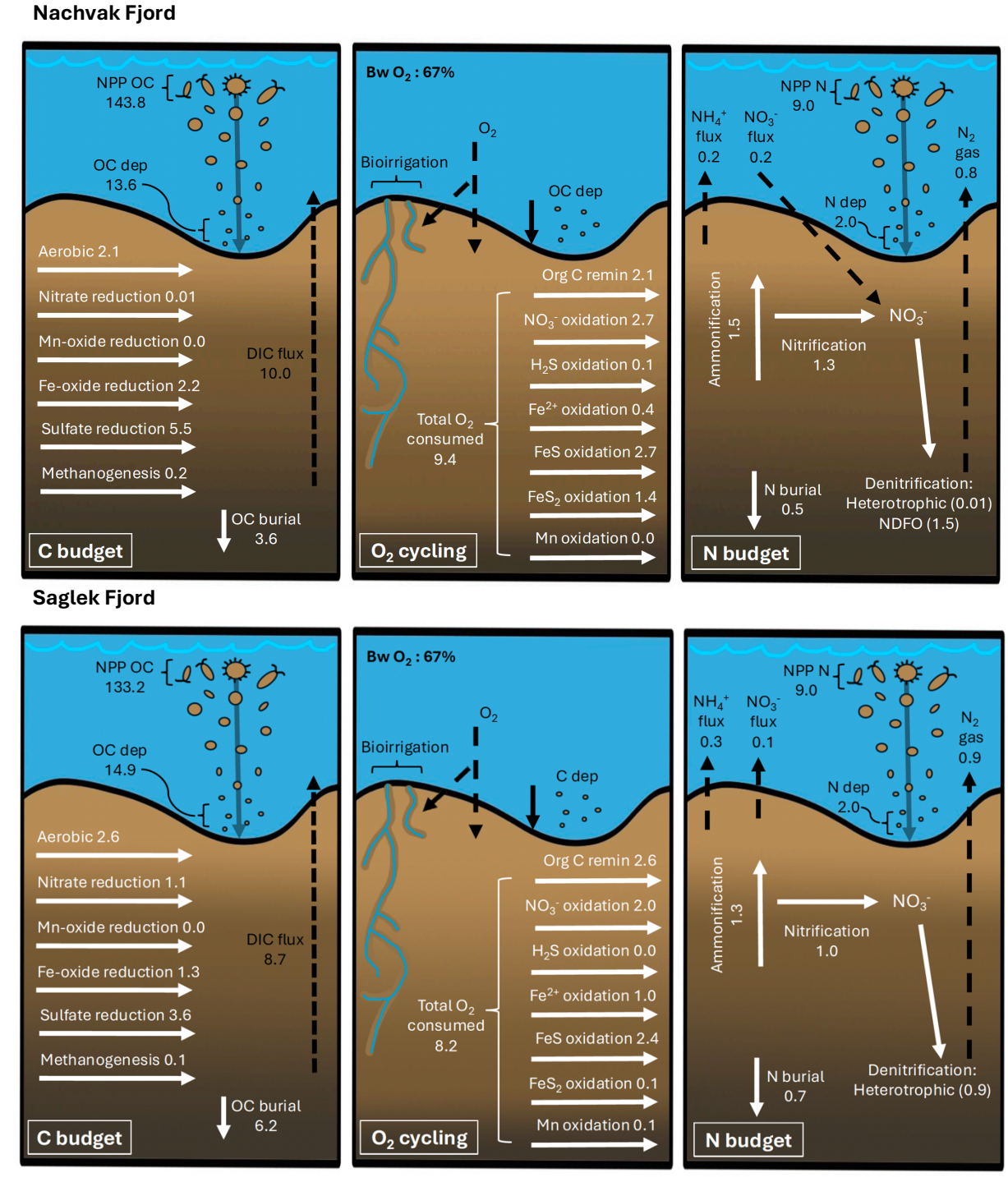

Figure 11. C budget, oxygen cycling, and nitrogen budget for sediments from Nachvak and Saglek fjords in mmol m^{-2} d^{-1}.

https://doi.org/10.5194/egusphere-2026-5292
Preprint. Discussion started: 9 September 2026

Our modelled estimates of OC deposition (13.6 mmol C m^{-2} d^{-1} and 14.9 mmol C m^{-2} d^{-1} for Nachvak and Saglek fjords, respectively) align with the global fjord average depositional OC rate estimate (often called OC accumulation rate: OC AR) of 12.3 mmol C m^{-2} d^{-1} (Smith et al., 2015). Both modelled burial efficiencies (Nachvak: 26%, Saglek: 42%), and especially Saglek Fjord, exceed published estimates from other fjords (4-25%) (Watts et al., 2024; Rakshit et al., 2025; Włodarska-Kowalczuk et al., 2019; Kuliński et al., 2014) underscoring the importance of Nunatsiavut fjord sediments for OC preservation. Based on published data (Simo-Matchim et al., 2016) on summer phytoplankton community and primary production (631.5 ± 14.6 g OC m^{-2} yr^{-1} and 584.0 ± 21.9 g OC m^{-2} yr^{-1} for Nachvak and Saglek fjords respectively) we calculated a C budget for each fjord (Figure 11) that estimates seafloor deposition rates of 9.5% and 11.0% of surface primary production at Nachvak and Saglek fjords, respectively. These deposition rates correspond to the lower end of expected export on continental shelf (Canfield, 1993: ~15-50%) and are lower than values reported for glaciated western Greenland fjords (Sørensen et al., 2015: ~52%).

Our regional estimate of OC burial for all northern Nunatsiavut fjords varied from 8,000-33,000 tonnes of OC yr^{-1}. Scottish and Irish fjord systems bury 57-107 tonnes of OC km^{-2} yr^{-1} (Smeaton and Austin et al., 2019), a substantially higher estimate than our calculated OC burial in northern Nunatsiavut fjords in this study (9.4-38.9 tonnes of OC km^{-2} yr^{-1}). Muddy sediments for both Irish and Scottish fjords cover ~1159 km^2 (Smeaton and Austin et al., 2019) compared to our area of 849 km^2, although surface sediments of Scottish fjords contain OC up to ~10 wt%, an average of ~3 wt% (n=356) and a sedimentation rate range of 0.15-0.33 (n=15; Smeaton et al., 2021). Although Scottish fjords share a similar latitude with Nunatsiavut fjords (~56 ºN), Scottish fjords have shallow and flat bathymetry and do not freeze in the winter – features that likely enhance annual surface production and terrestrial OM and riverine input, thus increasing potential burial. Similarly, burial rates in some Norwegian fjords (13-171 g OC m^{-2} yr^{-1}) also exceed rates in our study likely because of their denser vegetation, limited freezing, and restriction of basin and fluvial transport (Duffield et al., 2017).

Most studies of OC burial rates measure different sediment depths with varying sedimentation rates, complicating intercomparisons. As per our model results, remineralization rates of OC slow considerably below the bioturbated zone but never reach 0, demonstrating ongoing degradation even below the mixed depth, albeit slowly. Bradley et al, (2022) noted that burial rates often neglect this degradation at depth and instead encourage the use of transfer or burial efficiencies with age that clearly define sediment depth. Using this approach, we infer that OC buried in Nachvak Fjord and Saglek Fjord sediments can persist for at least ~200 years at a sediment depth of 50 cm. Burial efficiencies for sediment from both fjords decrease rapidly from 0-50 years and then remain fairly stable from 50-200 years (Figure 10).

The need to adjust some nitrogen cycling rates for both models may underscore the importance of those processes for our benthic-pelagic cycling. When modelled C/N ratios matched data, between ~6-8 for both sites, we overestimated NH_4^+ fluxes by 4X their observed rates (see supplementary material). To reduce the NH_4^+ fluxes and to simulate observed NO_3^- fluxes, we

https://doi.org/10.5194/egusphere-2026-5292
Preprint. Discussion started: 9 September 2026

increased nitrification rates (model parameter: k.no3 in $mmoles^{-1}$ yr^{-1}) for both models but notably more so for Nachvak Fjord. This adjustment alone enabled the Saglek Fjord model to simulate data well, however, our model still underestimated Nachvak Fjord NO_3^- flux. Increasing the nitrate-dependent iron oxidation rate (NDFO, model parameter: k.Fe2.no3 in $mmoles^{-1}$ yr^{-1}) rate parameter in the Nachvak Fjord model resulted in a good model fit to the observed NO_3^- flux and Fe^{2+} porewater concentrations well (see supplementary material). Relatively low TOC concentrations might shift denitrification to being less dependent on organic compounds as electron donors (heterotrophic) to favouring denitrification that use other reliable energy sources like reduced metal oxides which have been associated with outer fjord locations (Middelburg et al., 1996; Laufer et al., 2021).

Microbial community structure assessments provide additional support for the prevalent biogeochemical processes in these fjord sediments. Nachvak Fjord sediments were predicted to have fewer denitrifiers based on inferred prevalence of the narG gene marker (Fig. 9), in agreement with modelled metabolisms (Fig. 7). Saglek Fjord sediment is predicted to have fewer sulfate reducers based on inferred prevalence of the dsrA gene marker, coinciding with lower sulfate reduction rates in the Saglek Fjord model compared to the Nachvak Fjord model. Comparing the napA marker between both fjords predicted a higher relative abundance in Nachvak Fjord compared to Saglek Fjord sediments. Previous studies report the napA marker in microbial communities capable of performing both heterotrophic denitrification and NDFO (Chen et al., 2022). We note that NDFO can be mixotrophic, requiring an organic co-substrate but some studies provide evidence of autotrophic organisms when abundant NO_3^- and Fe^{2+} coincide with very low (<1%) TOC (Laufer et al., 2016). Our model was unable to resolve increased porewater NO_3^- concentrations in Nachvak Fjord sediment, despite observing *Thioploca*, *Beggiatoa,* or foraminiferal communities in 16S rRNA gene sequencing data that other studies associate with higher porewater NO_3^- (Thamdrup and Canfield, 1996; Bohlen et al., 2011; Rakshit et al., 2025), they occurred in very low relative abundances (<1%).

The adapted Nachvak Fjord model contributed 0.4% of OC degradation to heterotrophic denitrification whereas the Saglek Fjord model attributed ~13.5% to heterotrophic denitrification. The modelled N budget for Nachvak Fjord sediments indicates that nitrification oxidizes most NH_4^+ from ammonification to NO_3^-, which then enables Fe^{2+} oxidation through NDFO. In contrast, in Saglek Fjord sediment, more NH_4^+ effluxes out of sediment and the remainder used to produce NO_3^- that almost entirely undergoes heterotrophic denitrification via OM oxidation. Sediment from both fjords represents a dominant N sink using denitrification pathways (linked to organic carbon or reduced iron oxide substrates) that exceeds N lost through burial. These results contrast with those reported by Cheung et al. (2026) that N burial represents the dominant N sink for fjords globally but especially in ventilated, cold, high latitude fjords. Despite well-oxygenated (~67% O_2 sat) and cold (<1 ºC) fjord basins in our study, sediment samples and resulting model simulations demonstrated stronger denitrification compared to burial for both sites, suggesting that temperature and bottom water O_2 alone may not determine N removal. In our study, higher nitrification rates might link to enhanced denitrification. These results highlight the utility of pairing point-based measurements, diagenetic modelling, and 16S genomic data to observe benthic-pelagic processes locally.

https://doi.org/10.5194/egusphere-2026-5292
Preprint. Discussion started: 9 September 2026

Developing regional scale estimates of OC storage and inventories in coastal environments, such as fjords, require suitable sampling coverage to capture the diversity of depositional environments in a region. On the one hand, this coverage often entails combining numerous discrete sediment samples (grabs, sediment cores) analysed for a limited number of variables, such as OC content, often paired with continuous datasets such as multibeam bathymetry or backscatter. On the other hand, linking C with other important biogeochemical cycles, such as oxygen or nitrogen, requires detailed process-based measurements (e.g., fluxes, porewater chemistry) of a sufficient number of components within each cycle. To quantify the ecosystem services that these biogeochemical cycling hotspots provide requires both types of measurements. However, seasonal ice coverage and substantial logistical costs in remote environments create significant challenges, such as the Arctic or subarctic. Our study attempts to strike a balance between these two goals by conducting process-based studies in two sites within two fjords along the Nunatsiavut coast, in the eastern subarctic, Canada.

Previous burial rates in fjords globally were calculated with minimal fjord sampling coverage and assuming consistent sediment composition throughout fjord basins (Smith et al., 2015). Other studies then used inventories to refine the composition of fjord sediments in relation to OC content (Smeaton and Austin, 2019). Subsequent studies have described fjord sediments as heterogenous in terms of grain size, OC content, and depositional settings (Smeaton and Austin, 2019) highlighting how sampling location can vastly change estimates of OC sequestered on a fjord scale, as we infer in our study. Although our two sampling sites capture some of that variability with their distinct benthic-pelagic cycling, greater sampling coverage could improve our estimate when considering fjords along the Nunatsiavut coastline as an important region for OC burial. Our model results also demonstrate weighted contributions of pathways responsible for OC breakdown can vary with OC content and nutrient cycling. Nevertheless, these burial rates do not result in permanently stored OC; degradation continues slowly after the bioturbated depth. Moreover, the burial rates themselves vary.

Retreating glaciers, invasion of new vegetation, and alterations to seasonality of sea ice coverage are causing rapid changes in mid-high latitude fjords; all could influence the amount of OC delivered to the seafloor, the quality of that OM, how much remains sequestered, and the timescale of that burial. Our study compared metabolisms within sediments from two subarctic fjords with ongoing climate-related transitions. Our modelled results point to nitrification in these fjords as a significant process, potentially leading to denitrification as the stronger removal pathway, even in these well-ventilated basins. As known OC burial hotspots, fjords provide an important ecosystem service, highlighting the importance of regional estimates in improving our understanding of this C sink. Nonetheless, we suggest pairing these rates with local process-based measurements, including a variety of biogeochemical variables across cycles, and modelling to assess further how these environments might continue to respond to the current warming regime.

https://doi.org/10.5194/egusphere-2026-5292
Preprint. Discussion started: 9 September 2026

5 Conclusions

Our study provides the first calculated OC burial rates in fjord sediments along the Nunatsiavut (Labrador) coast, Canada. We demonstrate the utility of a holistic approach to sediment geochemistry combining geochemical observations, diagenetic modelling and 16S rRNA gene amplicon sequencing to validate model results. Using a diagenetic model, we broke down the composition of metabolisms responsible for OC degradation and observed low rates (<1%) of heterotopic denitrification in Nachvak Fjord sediments despite elevated NO_3^- in porewater samples. In contrast, Saglek Fjord yielded high rates (~13.5%) compared to other studies. Model adjustments suggest Nachvak Fjord sediments may instead prioritize nitrate-dependent iron oxidation to remove N, although both models indicate that denitrification (heterotrophic or nitrate-dependent iron oxidation) exceeds burial. Differences in benthic metabolisms likely reflect sampling fjord location, which influences the availability of OC and iron cycling within sediments. Our nitrogen budgets suggest Saglek Fjord sediments may be a more efficient N sink in burying ~2X more OC annually compared to Nachvak Fjord sediments, though more sampling would better capture sediment heterogeneity within these fjords. With our measurements, we were able to model benthic metabolisms in sediments from both fjords that match predicted functional potential derived from microbial biodiversity profiling. Our model adaptations also highlight that nitrification could be an important process in well-ventilated fjords, resulting in more N removal through dentification (heterotrophic or nitrate-dependent iron oxidation). We estimate an OC burial rate of all northern Nunatsiavut fjords at 8,000-33,300 tonnes OC annually, which persists in the geological record for at least ~200 years.

Code and data availability

Data will be available through Fig Share. Model code will be available through Zenodo.

Author contributions

HDG: Conceptualization, Formal Analysis, Investigation, Methodology, Visualization, Funding acquisition, Writing – original draft, Writing – review & editing. FB: Investigation, Formal Analysis, Writing – original draft, Writing – review & editing. AN: Methodology, Writing – review & editing. MA: Formal Analysis. SH: Formal Analysis, Writing – review & editing. SWJ: Formal Analysis, Writing – review & editing. CH: Resources, Writing – review & editing. KAS: Writing – review & editing. PVRS: Writing – review & editing. CWH: Resources, Formal Analysis, Writing – review & editing. MS: Resources. RL: Resources. CA: Conceptualization, Investigation, Methodology, Funding acquisition, Supervision, Writing – review & editing.

Competing interests

The contact author has declared that none of the authors have competing interests.

https://doi.org/10.5194/egusphere-2026-5292
Preprint. Discussion started: 9 September 2026

Disclaimer

Copernicus Publications remains neutral with regard to jurisdictional claims made in the text, published maps, institutional affiliations, or any other geographical representation in this paper. While Copernicus Publications makes every effort to include appropriate place names, the final responsibility lies with the authors. Views expressed in the text are those of the authors and do not necessarily reflect the views of the publisher.

Acknowledgements

The authors extend gratitude to the Nunatsiavut Government, CCGS *Amundsen* crew and Amundsen Science. We also thank Claire Normandeau (Dalhousie CERC.OCEAN) and Anadiuska Natasha Rondón Vivas for their analytical assistance (Dalhousie CERC.OCEAN).

Financial support

This research has been supported by the Natural Sciences and Engineering Research Council of Canada (NSERC) Discovery Grant program (CA, PS), Dalhousie Universities' Ocean Frontier Institute (OFI), Ammundsen Science, and the Nunatsiavut government. Graduate student funding to HDG was provided through a NSERC PGS-D scholarship program, a Nova Scotia Graduate Scholarship, and the OFI Ocean Graduate Excellence Network (OGEN) in partnership with Fisheries and Ocean Canada's Grants and Contributions program. Additionally, FB was supported by the Nunatsiavut Government.

References

Apprill, A., McNally, S., Parsons, R., & Weber, L. (2015). Minor revision to V4 region SSU rRNA 806R gene primer greatly increases detection of SAR11 bacterioplankton. *Aquatic Microbial Ecology 75,* 129–137. https://doi.org/10.3354/ame01753.

Arctic Monitoring and Assessment Programme (AMAP). (2017). Snow, Water, Ice and Permafrost in the Arctic (SWIPA). Oslo, Norway, 269pp.

Atwood, T. B., Witt, A., Mayorga, J., Hammill, E., & Sala, E. (2020). Global patterns in marine sediment carbon stocks. *Frontiers in Marine Science*, *7*. https://doi.org/10.3389/fmars.2020.00165.

Boudreau, B. P. (1997). *Diagenetic models and their implementation: modelling transport and reactions in aquatic sediments*. https://www.researchgate.net/publication/235335761.

Bell, T., Devillers, R., & Edinger, E. (2009). Abstract: Application of multibeam sonar technology for benthic habitat mapping in Newfoundland and Labrador. In *Spring Technical Meeting Atlantic Geology 45*(1).

https://doi.org/10.5194/egusphere-2026-5292
Preprint. Discussion started: 9 September 2026

Bentley, S. J., & Kahlmeyer, E. (2012). Patterns and mechanisms of fluvial sediment flux and accumulation in two subarctic fjords: Nachvak and Saglek Fjords, Nunatsiavut, Canada. *Canadian Journal of Earth Sciences*, *49*(10), 1200–1215. https://doi.org/10.1139/E2012-052.

Berg, P., Risgaard-Petersen, N., & Rysgaard, S. (1998). Interpretation of measured concentration profiles in sediment pore water. *Limnology and Oceanography*, *43*(7), 1500–1510. https://doi.org/10.4319/lo.1998.43.7.1500.

Bianchi, T. S., Arndt, S., Austin, W. E. N., Benn, D. I., Bertrand, S., Cui, X., Faust, J. C., Koziorowska-Makuch, K., Moy, C. M., Savage, C., Smeaton, C., Smith, R. W., & Syvitski, J. (2020). Fjords as Aquatic Critical Zones (ACZs). In *Earth-Science Reviews*, *203*. https://doi.org/10.1016/j.earscirev.2020.103145.

Bohlen, L., Dale, A.W., Sommer, S., Mosch, T., Hensen, C., Noffke, A., Scholz, F. & Wallmann, K. (2011). Benthic nitrogen cycling traversing the Peruvian oxygen minimum zone. *Geochim. Cosmochim. Acta, 75*, 6094–6111.

Bradley, J. A., Hülse, D., LaRowe, D. E., & Arndt, S. (2022). Transfer efficiency of organic carbon in marine sediments. *Nature Communications*, *13*(1). https://doi.org/10.1038/s41467-022-35112-9.

Broenkow, W. W., & Cline, J. D. (1969). Spectrophotometric determination of hydrogen sulfide in natural waters. *Liminology and Oceanography*, *14*(3), 454-458.

Burdige, D. J. (2005). Burial of terrestrial organic matter in marine sediments: A re-assessment. *Global Biogeochemical Cycles*, *19*(4). https://doi.org/10.1029/2004GB002368

Callahan, B. J., McMurdie, P. J., Rosen, M. J., Han, A. W., Johnson, A. J. A., & Holmes, S. P. (2016). DADA2: High-resolution sample inference from Illumina amplicon data. *Nat Methods 13*, 581–583. https://doi.org/10.1038/nmeth.3869.

Canfield, D. E., Jorgensen, B. B., Fossing, H., Glud, R., Gundersen, J., Ramsing, N. B., Thamdrup, B., Hansen, J. W., Nielsen, L. P., Hall, P. O. J., Canfield, A., Nielsen, J. W., & Hall, L. P. (1993). Pathways of organic carbon oxidation in three continental margin sediments. In *Marine Geology, 113*.

Chen, X., Liu, C., Zhu, B., Wei, W. & Sheng, R. (2022). The contribution of nitrate dissimilation to nitrate consumption in *narg*- and *napa*-containing nitrate reducers with various oxygen and nitrate supplies. *Microbiol Spectr, 10*. https://doi.org/10.1128/spectrum.00695-22.

Cheung, H.L.S., Levin, L.S., Smeaton, C. Politi, T., Thamdrup, B., Santos, I.R. & Bonaglia, S. (2026). Long-term nitrogen burial exceeds denitrification in global fjords. *Nat Commun 17*, 3148. https://doi.org/10.1038/s41467-026-71116-5.

Cui, X., Bianchi, T. S., Savage, C., and Smith, R. W. (2016). Organic carbon burial in fjords: terrestrial versus marine inputs. *Earth Planet. Sci. Lett. 451*, 41–50. doi: 10.1016/j.scitotenv.2018.04.242

Dickson, A.G., Sabine, C.L. & Christian, J.R. (2007). Guide to best practices for ocean CO2 measurements. PICES Special Publication 3, 191 pp.

Dixon, P. (2003). VEGAN, a package of R functions for community ecology. *Journal of Vegetation Science 14*, 927–930. https://doi.org/10.1111/j.1654-1103.2003.tb02228.

https://doi.org/10.5194/egusphere-2026-5292
Preprint. Discussion started: 9 September 2026

Douglas, G.M., Maffei, V.J., Zaneveld, J.R., Svetlana, N.Y., Brown, J.R., Taylor, C.M., Huttenhower, C., Langille, M.G.I. (2020). PICRUST2 for prediction of metagenome functions. *Nature Biotechnology*, *38*, 685-688. https://doi.org/10.1038/s41587-020-0548-6.

Duffield, C.J., Alve, E., Andersen, N., Andersen, T.J., Hess, H. & Strohmeier, T. (2017). Spatial and temporal organic carbon burial along a fjord to coast transect: A case study from Western Norway. *The Holocene, 27*(7), 1325-1339. https://doi.org/10.1177/0959683617690588.

Faust, J. C., & Knies, J. (2019). Organic matter sources in North Atlantic fjord sediments. *Geochemistry, Geophysics, Geosystems*, *20*(6), 2872–2885. https://doi.org/10.1029/2019GC008382

Glud, R.N. *(2008).* Oxygen dynamics of marine sediments. *Marine Biology Research, 4,* 243-289. https://doi.org/10.1080/17451000801888726.

Hunt, C. W., Salisbury, J. E., & Vandemark, D. (2014). CO2 input dynamics and air-sea exchange in a large New England estuary. *Estuaries and Coasts*, *37*(5), 1078–1091. https://doi.org/10.1007/s12237-013-9749-2

Iversen, M. H. (2023). Carbon export in the ocean: a biologist's perspective. *The Annual Review of Marine Science, 15*, 357-381. https://doi.org/10.1146/annurev-marine-032122.

Jørgensen BB., Glud RN. & Holby O. (2005). Oxygen distribution and bioirrigation in Arctic fjord sediments (Svalbard, Barents Sea). *Mar. Ecol. Prog. Ser., 292*, 85 95. https://doi.org/10.3354/meps292085.

Jørgensen, B.B. & Kasten, S. (2006). Sulfur cycling and methane oxidation. In Marine Geochemistry Springer-Verlag, Berlin/Heidelberg, pp. 271–309.

Juul-Pedersen, T., Arendt, K.E., Mortensen, J., Blicher, M.E., Søgaard, D.H. & Rysgaard, S. (2015). Seasonal and interannual phytoplankton production in a sub-arctic tidewater outlet glacier fjord, SW Greenland. *Mar. Ecol. Prog. Ser. 524*, 27–38. http://dx.doi.org/10.3354/meps11174.

Kuliński, K., Kędra, M., Lege˙zy´nska, J., Gluchowska, M. & Zaborska, A. (2014). Particulate organic matter sinks and sources in high Arctic fjord. *J. Mar. Syst*., 139, 27–37.

Lindahl, O., Belgrano, A., Davidsson, L. & Hernroth, B. (1998). Primary production, climatic oscillations, and physico-chemical processes: the Gullmar Fjord time-series data set (1985–1996). *ICES J. Mar. Sci.* 55, 723–729.

Martin, M. (2011). Cutadapt removes adapter sequences from high-throughput sequencing reads. *EMBnet.Journal*, *17*(1), 10. https://doi.org/10.14806/ej.17.1.200.

Meyers, P.A. (1994). Preservation of elemental and isotopic source identification of sedimentary organic matter. *Chemical Geology*, **114**, 289–302.

McGrath, T., Cronin, M., Kerrigan, E., Wallace, D., Gregory, C., Normandeau, C., & McGovern, E. (2019). A rare intercomparison of nutrient analysis at sea: Lessons learned and recommendations to enhance comparability of open-ocean nutrient data. *Earth System Science Data*, *11*(1), 355–374. https://doi.org/10.5194/essd-11-355-2019

McMurdie, P. J., & Holmes, S. (2013). phyloseq: An R Package for Reproducible Interactive Analysis and Graphics of Microbiome Census Data. *PLOS ONE 8*, e61217. https://doi.org/10.1371/journal.pone.0061217.

https://doi.org/10.5194/egusphere-2026-5292
Preprint. Discussion started: 9 September 2026

Middelburg, J.J., Soetaert, K., Herman, P.M.J. & Heip, C.H.R. (1996). Denitrification in marine sediments: a model study. *Global biogeochemical cycles, 10(*4), 661-673.

Nittrouer, C. A., Sternberg, R. W., Carpenter, R., & Bennett, J. T. (1979). The use of pb-210 geochronology as a sedimentological tool: application to the washington continental shelf. *Marine Geology*, *31*.

Nittrouer, C.A., DeMaster, D.J., McKee, B.A., Cutshall, N.H., & Larsen, I.L. 1984. The effect of sediment mixing on 210Pb accumulation rates for the Washington Continental shelf. *Marine Geology, 54*(3–4): 201–221. doi:10.1016/0025-3227(84)90038-0.

Posit team (2025). RStudio: Integrated Development Environment for R. Posit Software, PBC, Boston, MA. http://www.posit.co/

Quast, C., Pruesse, E., Yilmaz, P., Gerken, J., Schweer, T., Yarza, P., et al. (2013). The SILVA ribosomal RNA gene database project: improved data processing and web-based tools. *Nucleic Acids Research 41*, D590–D596. https://doi.org/10.1093/nar/gks1219.

R Core Team. (2025). R: A language and environment for statistical computing. R Foundation for Statistical Computing (Version 4.5.0). *R Foundation for Statistical Computing*. https://www.R-project.org/

Rakshit, S., Glock, N., Dale, A. W., Armstrong, M. M. L., Scholz, F., Mutzberg, A., & Algar, C. K. (2025). Foraminiferal denitrification and deep bioirrigation influence benthic biogeochemical cycling in a seasonally hypoxic fjord. *Geochimica et Cosmochimica Acta*. https://doi.org/10.1016/j.gca.2024.10.010.

Roco, C.A., Bergaust, L.L., Shapleigh, J.P. & Yavitt, J.B. (2016). Reduction of nitrate to nitrite by microbes under oxic conditions. *Soil Biol Biochem 100,* 1–8. https://doi.org/10.1016/j.soilbio.2016.05.008.

Rysgaard, S., Glud, RN., Rysgaard-Petersen, N. & Dalsgaard, T. (2004). Denitrification and anammox activity in Arctic marine sediments. Limnol. Oceanogr., *49*(5), 1493-1502.

Santillano, D., Boetius, A. & Ramette, A. (2010). Improved *dsrA*-based terminal restriction fragment length polymorphism analysis of sulfate-reducing bacteria. *Appl Environ Microbiol 76*. https://doi.org/10.1128/AEM.03004-09.

Sauerland, L., Wegner, R., Moise, A., Kohl, L., Gil, J. & Wild, B. (2025). Vegetation type influences particulate organic matter storage along a low Arctic vegetation gradient. *Biogeochemistry, 168(6)*. https://doi.org/10.1007/s10533-025-01294-9.

Simo-Matchim, A-G., Gosselin, M., Blais, M., Gratton, Y. and Tremblay, J-É. (2016). Seasonal variations of phytoplankton dynamics in Nunatsiavut fjords (Labrador, Canada) and their relationships with environmental conditions. *Journal of Marin Systems*, *156*: 56-75. http://dx.doi.org/10.1016/j.jmarsys.2015.11.007.

Soetaert, K., Herman, P. M. J., & Middelburg, J. J. (1996). A model of early diagenetic processes from the shelf to ahyssal depths. *Geochimica et Cosmochimica Acta*, 60(6).

Solorzano, Lucia. (1969). Determination of ammonia in natural waters by the phenolhypochlorite method. *Limnology and Oceanography 14*(5), 799-801.

https://doi.org/10.5194/egusphere-2026-5292
Preprint. Discussion started: 9 September 2026

Sørensen, H.L., Meire, L., Juul-Pedersen, T., de Stigter, H.C., Meysman, F.J.R., Rysgaard, S., Thamdrup, B. & Glud, R.N. (2015). Seasonal carbon cycling in a Greenlandic fjord: an integrated pelagic and benthic study. *Mar. Ecol. Prog. Ser. 559*: 1-17/ https://doi.org/10.3354/meps11503.

Smith, R. W., Bianchi, T. S., Allison, M., Savage, C., & Galy, V. (2015). High rates of organic carbon burial in fjord sediments globally. *Nature Geoscience*, *8*(6), 450–453. https://doi.org/10.1038/NGEO2421.

Syvitski, J., Andrews, J.T., Scaher, C.T. & Stravers, J.A. (2022). Sediment fill of Baffin Island fjords: Architecture and rates. *Quaternary Science Reviews, 284*: 107474. https://doi.org/10.1016/j.quascirev.2022.107474.

Thamdrup B. & Canfield D. E. (1996). Pathways of carbon oxidation in continental margin sediments off central Chile. *Limnol. Oceanogr., 41*, 1629-1650.

Viollier, E., Inglett, P. W., Hunter, K., Roychoudhury, A. N., & Van Cappellen, P. (2000). The ferrozine method revisited: Fe(II)/Fe(III) determination in natural waters. *Geochemistry, 15*, 785-790.

Watts, E., Hylén, A., Hall, P., Eriksson, M., Robertson, E., Kenney, W., & Bianchi, T. (2024). Burial of organic carbon in Swedish fjord sediments: Highlighting the Importance of Sediment Accumulation Rate in Relation to Fjord Redox Conditions. *Journal of Geophysical Research: Biogeosciences*. *129*. https://doi.org/10.1029/2023JG007978.

Wickham, H. (2016). ggplot2: elegant graphics for data analysis., Second edition. Cham: Springer international publishing.

Wickham, H., Averick, M., Bryan, J., Chang, W., McGowan, L. D., François, R., et al. (2019). Welcome to the Tidyverse. *Journal of Open Source Software 4*, 1686. https://doi.org/10.21105/joss.01686.

Włodarska-Kowalczuk, M., Mazurkiewicz, M., G.rska, B., Michel, L. N., Jankowska, E., & Zaborska, A. (2019). Organic carbon origin, benthic faunal consumption, and burial in sediments of Northern Atlantic and Arctic fjords (60–81ÅãN). *Journal of Geophysical Research: Biogeosciences*, *124*(12), 3737–3751. https://doi.org/10.1029/2019JG005140.